Vernacular Caramel´s Adobe Masonry Dwellings - Material Characterization

Adriana Silva[1], Inês Oliveira[1], Vítor Silva[1] , José Mirão[2], Paulina Faria[3]

(1) Department of Civil Engineering, FCT, NOVA University of Lisbon, Portugal, adrianacostaasilva@gmail.com, ines.carvalholiveira@gmail.com, vmd.silva@fct.unl.pt

(2) Hercules Laboratory, Department of Geosciences, University of Évora, Portugal, jmirao@uevora.pt

(3) CERIS and Department of Civil Engineering, Faculty of Sciences and Technology, NOVA University of Lisbon, 2829-516, Caparica, Portugal; E-mail: paulina.faria@fct.unl.pt (corresponding author)

.ABSTRACT

In Pinhal Novo, Palmela, and neighboring municipalities, southern Lisbon region, there are a great number of small adobe masonry dwellings, made in the first half of the 20th century. The vernacular dwellings were constructed by families that came from the north/center region of Portugal to work at the local manors, and were called Caramel´s. Adobe samples from three of these dwellings were collected in Pinhal Novo and Moita, and tested for particle size distribution, X-ray diffraction, color, bulk density, ultrasonic pulse velocity, thermal conductivity, dry abrasion, flexural and compressive strength, capillary absorption and drying. It was possible to conclude that the adobe was not chemically stabilized and had no vegetable fibers. Average values for the adobe properties were defined and results were analyzed, revealing comparable to unstabilised adobe and even to lime stabilized adobe from other regions. The data on Caramel´s adobe can support the design of interventions to preserve at least some of these Caramel´s vernacular dwellings.

Keywords: Caramel´s culture; earth construction; laboratory characterization; in situ sampling; mechanical characterization; physical characterization; vernacular architecture

1. Introduction

Old adobes are masonry blocks or units, produced from plastic earth mortars introduced manually into wooden molds. They are demolded after initial drying (Parracha et al., 2019) and, after complete drying, they are used in the making of load bearing masonry walls (EN 1996-1-1, 2005). Vernacular adobe was made with just raw earth, usually without very coarse gravel, sometimes adding straw or sandy earth when the earth was too clayish. The addition of air lime to the plastic earth mortar could occur when the earth had low clay content, with the objective of producing adobe less vulnerable to water (Costa et al., 2013; Caporale et al., 2015) As old adobe was mainly unstabilized and vulnerable to water, remains of archaeological adobe were very difficult to

identify and could only be preserved when a fire took place, whether by accident or not. Otherwise, adobe was hard to be clearly distinguished from the surrounding earth materials in archaeological excavations. Nevertheless, archaeological constructions with adobe masonry were found in Mureybet and Jerf el Ahmar (Síria), dated from 10.000-8.000 B.C. (Cauvin, 1994). In Portugal, adobe was found at Alto do Outeiro, Baleizão, Beja district (Bruno, 2007) dated from 4000-3000 B.C.

Until the end of the first half of the 20th century, adobe masonry construction was very popular in several regions of Portugal, being used for external and internal walls, as is the case of the Aveiro (Silveira, Varum, and Costa, 2016) or Leiria region (Parracha et al., 2019). Masonries were also layered with an earth mortar, similar to the material of the adobe masonry, with the objective of achieving a better interaction between the different materials (Costa et al., 2018).

Despite the fact adobe construction experienced a decreased interest due to new methods of construction, in recent decades there has been a growing interest in earth construction technologies, mainly due to ecological and technical reasons. If earth buildings are well maintained, primarily by avoiding the access of water from rain and effective drying of moisture from indoor activities and from capillary rise, these constructions can last for long (Beckett et al., 2020) and the walls are completely recyclable at the end of their lifecycle, presenting both economic and environmental benefits (Bui and Morel, 2015).

Another aspect is related to the hygrothermal properties. In fact, due to the clay content, earthen construction products present a very high hygroscopic capacity, capturing and releasing indoor moisture, being able to passively contribute to equilibrate indoor relative humidity and, therefore, hygrothermal environment (Fabbri et al., 2017; Lima et al., 2020). Furthermore, earth walls present high mass and, therefore, thermal inertia, which is extremely important in Mediterranean regions, with high daily thermal amplitudes and opportunity to achieve night cooling during the hot season, along with good acoustic insulation. According to Costa et al. (2018) adobe walls should maintain their significant thickness in order to obtain the best mechanical and thermal properties.

All these concerns, together with social and cultural aspects, contribute to an increased motivation to preserve vernacular earthen dwellings, since they represent a valuable architectural heritage.

Due to the increase in comfort requirements in the past decades, pure conservation of the dwellings may not be enough in cases where there is a need to proceed with rehabilitation. In several regions of Portugal, there are a significant number of adobe buildings in need of conservation and rehabilitation, with recent research taking place with the objective of giving a new life to these buildings (Costa et al., 2018; Parracha et al., 2019). To support interventions of conservation and rehabilitation there is a need to access the characteristics of the materials by experimental methods. A synthesis of material characterization of Portuguese adobe masonry can be found in Table 1.

Table 1. Synthesis of material characterization of vernacular adobe masonry in Portugal.

Reference	Location	Sample	Typology	Density (kg/m³)	Compressive strength (N/mm²)	Flexural strength (N/mm²)
Coroado et al. (2010)	Aveiro (dwellings)	MP11			0.51	-
		CS1			0.25	
		TM1			1.44	
		LMM3			0.41	
Silveira et al. (2012)	Aveiro (dwellings, interior wall)	H_01		-	1.24	0.13
		H_02			1.00	0.19
		H_03			0.75	0.19
		H_04			0.66	-
		H_05			2.15	-
		H_09			0.70	-
		H_10			1.98	-
		H_11			1.08	-
	Aveiro (walls dividing properties)	W_01			0.94	
		W_02			0.83	
		W_04			0.94	0.13
		W_05			1.72	0.12
		W_06			1.25	0.40
		W_07			0.80	-
		W_09			1.05	-
		W_10			0.98	-
Costa et al. (2013)	Aveiro, Anadia (dwellings)	A2-1	Air lime stabilized adobes		1.92	
		A2-2			2.05	
		A3-1			2.31	
		A3-4			2.09	
		A8-1			2.35	
		A8-2			2.55	
		A8-3			3.43	
		A8-4			3.58	
		A8-5			2.39	
	Aveiro, Murtosa (dwellings)	M1-2			1.87	
		M1-3			2.07	
		M1-4			1.61	
		M2-2			1.25	
		M2-3			1.64	
		M10-2			2.52	
		M10-3			1.4	
		M11-3			2.63	
		M11-5			1.93	
		M11-6			1.32	
Figueiredo et al. (2013)	Aveiro (wall built with material from traditional dwellings)	Adobes			0.46	0.15
Silveira, Varum and Costa (2013)	Aveiro, Bunheiro (dwellings)	H12_a02		1652	0.28	0.23
		H12_a03			1.02	-
		H12_a06			1.21	-
		H12_a08			-	0.98*
	Aveiro, Murtosa, (dwellings)	H13_a01		1530	-	0.03
		H13_a10			0.28	-
	Aveiro, Cacia (dwellings)	H20_a07		1540	0.23	-
Costa et al. (2019)	Aveiro (demolished vernacular dwellings - exterior walls)	Group 1			>1	-
		Group 2	Unstabilized adobes		1-2	>0.50
		Group 3	Unstabilised adobes with fibers		<2	-
Parracha et al. (2019)	Leiria (dwellings)	A1_A	Unstabilized adobes	1730	1.06	0.27
		A2_A		1400	0.69	0.11
		A3_A		1450		0.09

Notation: Aveiro is located in the North of Portugal while Leiria belongs to the Central region of the country; * - Average value, lower than the one mentioned (1.03 N/mm²), but even so high in comparison to other values.

Table 1 shows that some data exists on Aveiro region adobe and only one reference on Leiria region adobe. In terms of mechanical properties, the results of Table 1 allowed to divide adobe in three classes: class 1, gathering samples showing lower compressive strength (<1 N/mm^2); class 2 with those presenting medium compressive strengths (from 1–2 N/mm^2), and class 3 with those presenting higher compressive strengths (> 2 N/mm^2). The data also shows that there are two main types of vernacular adobes characterized in Portugal: unstabilized and air lime stabilized. The latter seems to be common in the Aveiro region, which can be justified by a region where low clay content earths predominate (Costa et al., 2019). However, the stabilization does not necessarily mean there is an associated higher strength in comparison to unstabilized adobe, as can be observed from Table 1. Nevertheless, it is expected that air lime stabilized adobe presents higher durability when in contact with water. Costa et al., (2019) refers that unstabilized adobes of the Portuguese Central Coast usually incorporated vegetable fibers, although no reference to this condition is presented in the characterization of Aveiro adobe (Coroado et al., 2010; Silveira, Varum and Costa, 2013; Costa et al., 2013; Figueiredo et al., 2013), except for the case of Silveira et al. (2012), that mentions the addition of fibers such as straw and sisal to the adobes.

In the south of river Tagus, south of Lisbon, Pinhal Novo parish, Palmela municipality, and neighboring municipalities, such as Moita, there are a great number of small adobe masonry dwellings, made in the first half of the 20th century. These vernacular dwellings were constructed by families that came from the north/center of Portugal to work at the manors located in this region (Fernandes, 2008; Sampaio, Oliveira and Faria, 2017) These people were called Caramel´s and associated with the Caramel culture. Therefore, the dwellings were named Caramel's dwellings. These dwellings are mainly composed by load bearing adobe masonry walls and a simple wooden roof structure, covered with ceramic tiles. The load bearing adobe walls were originally rendered and plastered. Most of these constructions are currently abandoned, needing major repair (Figure 1).

Figure 1. Exterior façade of a Caramel dwelling in Pinhal Novo, showing lack of protective render and degradation of adobe, by weathering and insects, showing the importance of a protective render.

The material characterization of the adobe, as well as a deeper knowledge of building technology, can contribute to support the repair methodology. Analyzing the literature (Table 1), no data on material characterization of adobe from the region of Pinhal Novo and Moita could be found. Therefore, an experimental campaign was held, based on the characterization of adobe samples collected from three Caramel´s dwellings.

2. Materials and methods

2.1. Case studies, samples and specimens

With the objective of proceeding with the characterization of the materials sampling was necessary, but authorization to collect adobe samples was difficult to obtain and only positive on three case studies: two of them located in Pinhal Novo parish, Palmela municipality (case 218 and 267) and one in Moita municipality (case 17015) (Figure 2). Two of the dwellings were in ruins and the third (17015) had been recently demolished (Table 2). Samples were collected from the three dwellings, between April and June 2017. Adobes were applied in the masonries with their second dimension defining the walls´ thickness (Figure 1).

Figure 2. Location of the three case studies in Moita municipality and Pinhal Novo parish, at the South bank of river Tagus, South Lisbon: dwellings 218, 267 and 17015.

On Table 2 the presentation of the dwelling's year of construction and municipality, exact location by GPS coordinates, an example of the collected adobe and the adobe dimensions (also measured in situ and not only on the collected samples), as well as the masonry joints thickness, can be consulted. There were a total of 22 collected samples from the three case studies: 10 from dwelling 218, 6 from dwelling 267 and 6 from dwelling 17015. Samples were given the number of the dwelling, plus a letter in alphabetical order (Table 2).

In the laboratory, the preparation of samples started with the removal of rendering, plastering and bedding joint mortars, with the help of a hammer and chisel. Examples of adobe with the original

dimensions of each case study were preserved, integrating the DB-HERITAGE project physical database (W1).

Table 2. Identification of the dwellings and samples collected.

Dwelling and number		Construction year and municipality	GPS coordinates	Adobe sample	Adobe dimensions and masonry joint thickness (m)	Sample ID
	218	1939, Pinhal Novo, Palmela	*38°37'04.8"N 8°52'36.3"W*		0.10x0.51x0,32 0.02-0.025	218_a 218_b 218_c 218_d 218_e 218_f 218_i 218_j
	267	1942, Pinhal Novo, Palmela	*38°37'9.51"N 8°54'30.07"W*		0.10x0.50x0,30 0.02-0.025	267_a 267_b 267_c 267_e 267_f 267_g 267-h
Demolished	17015	Unknown, Moita	*38°37'59.6"N 8°58'04.1"W*		0.10x0.51x0,38 0.02-0.025	17015_a 17015_b 17015_c 17015_d 17015_e 17015_f

Some tests were performed directly on the original adobe samples (Table 3), that were roughly the same size (Table 2), such as color assessment, ultrasonic pulse velocity, surface hardness by durometer and thermal conductibility. In a second phase, due to scarcity of samples and trying to adapt the best as possible to the tests, some of the original adobe samples were cut into cubic and rectangular specimens with the help of an electric saw (Figure 3). Samples with the dimensions of 0.10 m (adobe height) x 0.15 m x 0.30 m were used for the bulk density and flexural strength tests. Smaller cubic samples with the dimensions of 0.10 m (adobe height) x 0.15 m x 0.15 m were used for compression tests – individual sample testing and testing of two overlapped samples with bedding mortar.

Table 3. Standard or guideline and specimens from each case study used for each test.

Test (and guideline)	Specimen	218	267	17015
Color assessment (CIELAB system)	Adobe			
Material particle size distribution (EN 1015-1, 1999; Walker and Australia, 2002), Expedite sedimentation (Walker and Australia, 2002) and XRD	Adobe disaggregated material	-	-	-

Ultrasonic pulse velocity (EN 12504-4, 2004)	Adobe	218_a 218_b 218_c 128_d 218_e 218_g 218_h 218_g	267_a 267_b 267_c 267_d 267_e 267_f 267_g 267-h	17015_a 17015_b 17015_c 17015_d 17015_e 17015_f
Surface hardness by durometer (ASTM D2240-15, 2015)		218_a 218_b 218_c 218_c 218_d 218_e 218_f 218_g 218_h 218_i 218_j	267_a 267_b 267_c 267_d 267_e 217_f 267_g 267_h	17015_a 17015_b 17015_c 17015_d 17015_e 17015_f
Thermal conductibility (ASTM D5930-17, 2017)		218_a 218_b 218_c 218_d 218_e 218_f 218_g 218_h 218_i 218_j	267_a 267_b 267_c 267_d 267_e 267_f 267_g 267_h	17015_a 17015_b 17015_c 17015_d 17015_e 17015_f
Resistance to dry abrasion (DIN 18947, 2013)	Irregular adobe samples with a flat surface	218_1 218_2 218_3 218_4 218_5	267_1 267_2 267_3 267_4 267_5	17015_1 17015_2 17015_3 17015_4 17015_5
Capillarity (EN 15801, 2009 Drying (EN 16322, 2013)		218_1 218_2 218_3 218_5	267_1 267_2 267_3 267_4 267_5	17015_1 17015_2 17015_3 17015_4 17015_5
Bulk density (DIN 18946, 2013)	Prismatic cut sample 0.10 x 0.15 x 0.30 (m)	A_1 A_2 A_3 A_4 A_5 A_6 A_7	B_1 B_2 B_3 B_4 B_5 B_6	C_1 C_2 C_3 C_4 C_5 C_6
Flexural strength (Walker and Australia, 2002; EN 1015-1, 1999)		A_1 A_2 A_3 A_5 A_6 A_7	B_3 B_4 B_5 B_6 B_7	C_1 C_2 C_3 C_4 C_6
Compressive strength - simple specimens (NTE E.080, 2017; Walker and Australia, 2002; NTC 5324, 2004)	Prismatic resulting from flexural test cut with 0.10 x 0.15x 0.15 (m)	A_0.1 A_0.2 A_0.3 A_0.4 A_4.2 A_5.2 A_6.1	B_0.1 B_1.1 B_2.2 B_4.1 B_7.2	C_0.3 C_1.1 C_1.2 C_3.1 C_4.1 C_4.2 C_5.1
Compressive strength - two overlapped adobe specimens (NTE.E.080, 2017)	Specimens of two cut samples of 0.10 x 0.15 x 0.15 (m) with bedding mortar	A_1 A_2 A_7	B_3 B_5 B_6	C_0 C_2 C_6

Figure 3. Adobe samples cutting for specimen preparation.

The cutting was performed with the objective of creating regular size test specimens for some laboratorial testing.

For instance, from the original sample 17015_d (Table 2) a prismatic specimen of 0.10 m x 0.15 m x 0.30 m was cut out of the original sample and is designated by C_4 (Table 3), as well as sample C_0.3 with 0.10 m x 0.15 m x 0.15 m. From the disaggregated material, testing for material particle size distribution was performed, expedite sedimentation and X-ray diffraction. Samples and specimens obtained from each case study and used for each test are presented in Table 3, as well as the test standards or guidelines that were used.

2.2. Testing methods

2.2.1. Material characterization

As mentioned in Table 3, due to scarcity of sampling for all the testing campaign, the material characterization was performed with adobe portions that were not used for other tests, and that mainly resulted from cutting.

To understand if the adobes were unstabilized or stabilized with air lime (which is usual in some Portuguese regions, Table 1), a simple test of immersion in water was performed with small samples cut from them. The samples immediately dissolved, indicating that most probably they had no addition of lime, in opposition to what happens with several cases in the Aveiro region (Figueiredo et al., 2013; Silveira et al., 2012; Silveira, Varum, and Costa, 2013; Coroado et al., 2010).

Therefore, the testing campaign was defined based on that premise, namely the possibility to perform particle size distribution by disaggregated material and expedited sedimentation tests.

In an initial visual evaluation of the grain size, many differences were observed between the samples, namely in terms of major aggregate dimensions. It was also found that the organic matter in the earthen matrix was very scarce; only few roots and only in some cases.It seems to be

accidentally incorporated within the earthen material and not specifically added. Therefore, no plant fibers were used on the adobe production.

For all the following tests, the samples were maintained at a temperature of 23±2°C and relative humidity (RH) of 65±5%.

For particle size assessment, a 1 kg specimen representing the total sample was chosen for each case study. Clayish earth can only completely deagglomerates when in contact with water, which is the reason why the granulometric analysis of this type of material must be made by humid procedure. However, it was considered that there was not enough material to proceed with the wet particle size distribution and sedimentation test for the fine fraction. Therefore the dry grain size test was made base on EN 1015-1 (1999) by sieving. ASTM sieves 1''1/2, 1'', ¾'', ½'', 3/8'', nº4, 8, 16, 30, 50, 100 and 200 were used. At the end of the test, the loss of material throughout the testing was not superior to 1% of the total of the samples.

In parallel and to complement the analysis of the dry particle size distribution, and, an expedited sedimentation test was performed, generally designated as the jar sedimentation test based on HB 195 (Walker and Australia, 2002), to qualitatively provide the proportions of sand, silt and clay existing in the earthen samples.

After removing very coarse (thicker than sand) aggregates of a sample, it was placed material in a transparent glass jar with a straight base (that was previously made with a cement paste layer), mixed with water and let the particles to decant, so that the proportions of sand, silt and clay (that decant at different speeds and, therefore, form separate layers) can be determined: ¼ of the bottle capacity was filled with earth (125-135 g for each case study), ¾ with potable water. The bottle was shaken vigorously for 1 to 2 minutes and left to rest for an hour. One hour later it was shaken again. After some time, thick and thin sand, as well as silt were already visible. After 24 hours, clay particles could also be distinguished (Figure 4).

Figure 4. Expedited sedimentation test: a) start of the test; b) after 50 minutes.

Results were obtained by analysing at the 24 h mark the differences in height of the various layers and transforming them into percentages (Figure 5).
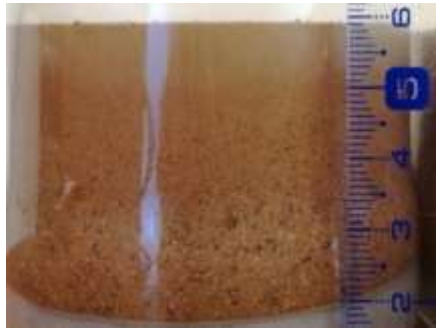
Figure 5. Assessment of sedimentation test results after 24 h of case study 218.

The X-ray diffraction (XRD) was performed with the objective of assessing, by comparison, the mineralogical characteristics of the earth that composed the adobe. A sample from the clayish matrix of each case study was selected, disaggregated, directly sieved through the sieve 200, with 0,075 mm of the ASTM series, and furthermore manually milled until a finer powder specimen was achieved. No further procedure (e.g. decantation, centrifugal processing) was applied for separating the silt and clay particles.

After this process, 2 g specimens were thus analyzed in Bruker D8 Discover diffractometer (Figure 6), equipped with a 1D lynxeye detector and using a Cu Kα radiation source (40 kV, 40 mA).

Figure 6. X-ray diffractometer "BrukerTM D8 Discover"

The diffractograms were registered between 3º and 75º, 2θ, with an increment of 0.05º 2θs-1. The identification of the materials was performed using software DIFFRAC.SUITE EVA and the database PDF- 2. The semi-quantitative abundance of minerals in the samples was obtained through the method of Reference Intensity Ratio (RIR) after Hubbard et al, 1976.

2.2.2. Adobe characterization

The tests performed to characterize the adobe are presented in Table 3, as well as the samples, standards and guidelines that were used. All the samples were in equilibrium at 23±2 °C and 65±5 % RH.

The color of the adobe was assessed through a colorimeter Konica Minota Chroma Meter Cr-400 that uses the CIELAB system. The color is tracked in three dimensions: a* (the axis between red

and green), and b* (between yellow and blue) - both axis vary between -128 and +128 - and L* represents the lightness of the color (and varies between 0 and 100).

The ultrasonic pulse velocity test has the objective of evaluating the compactness, homogeneity and eventual cracks in the material, through ultrasound. The indirect method was utilized, with the two transducers placed in the same face of the adobe. A Pundit equipment from Proceq was used with a frequency of 54 kHz. The first transducer was positioned in a fixed point, and three readings were made with the other three points, for a total of 4 points. The velocity of propagation of the ultrasound is calculated through the coefficient between the distance of the two-reading points and the time the wave takes to be recorded. The surface hardness test was performed with a Proced durometer Shore A, consisting of leaning the equipment to the surface of the adobe that is being evaluated. The pin is pressured perpendicularly to the surface of the adobe. The pressure applied makes the pointer move in a scale of 0 to 100, indicating the superficial resistance in face of the bolt penetration. In the surface of the sample, a mapping of the points to test, with 5 cm in between, was made and for each zone there were 5 readings. By the test of dry abrasion resistance, the wear imposed by 20 rotations brushing the surface is assessed, simulating abrasion of inhabitants indoor and particularly wind with suspended particles outdoors, when the adobe is not protected. A plastic brush of high hardness was used with a constant charge of 2 kg, being the loss of weight measured. To assess the thermal conductivity of the adobe they were previously stabilized at 23 ±2 °C and 65 ±5 % RH. A contact probe API 210412, with 6 mm of diameter and a measuring range of 0,3 – 2,0 W/(m.K), was applied on an ISOMET 2014 Heat Transfer Analyser equipment and placed in contact with the completely smooth surface of samples.

For the apparent bulk density determination of adobe samples, a digital caliper was used to measure the test specimen dimensions and the mass was registered with a precision scale of 0.1 g.

A Zwick-Rowell Z050 with a load cell of 50 kN and a displacement velocity of 1.5 mm/min was used to perform the flexural tests. Based on Walker and Australia (2002), a space between supports of 220 mm was adopted, having in consideration the smaller specimen to use in the test had 280 mm of length. Illampas, Ioannou, and Charmpis (2014) refer that even though there is not a pattern procedure to determine the flexural strength, the specimens should be tested in the direction they would function in the building. Therefore, the position of the tested specimens followed that indication.

The same Zwick-Rowell Z050 was used for the compressive tests. These were performed by two different test procedures: the testing of simple axial compression of adobe samples (Figure 7a) and the testing of specimens composed by two portions of adobe overlaid with a bedding mortar (Figure 7b). For both cases, due to the presence of aggregates of elevated dimensions, the choice was not to utilize the cubic specimens of 0.10 m x 0.10 m x 0.10 m, as indicated on the NTE E.080 (2017),

but larger and more representative samples, maintaining the original thickness of the adobe and making parallelepipeds with 0.15 m x 0.15 m x height of the adobe, that was 0.10 m for all the tested adobe (Table 3). However, this choice resulted on having adobe specimens for simple compressive test with height-to-width ratio of 0.7, that is lower than 1 and can, in turn, result to increased platen restrain effects that have to be taken in consideration when analyzing the results. This was also the motivation for, as complement of the simple compressive tests, performing also compressive test but with two overlapped adobe specimens with bedding mortar.

Figure 7. Compression test equipment for: simple specimens (a) and overlapped specimens with bedding mortar (b) showing the specimens top and bottom capping.

For the specimens composed by overlapped adobe samples, a mortar was made with the same earth of each case study, and placed in between the two samples, as a bedding mortar, in a similar way to Adorni, Coisson and Ferreti (2013). As the bedding mortars were applied with 1-2 cm thick, the coarser particles of the earthen materials not compatible with that thickness were previously removed. The water was added so the earth mortars present a workability considered adequate for bedding mortars. Immediately after its preparation, a fresh sample of each earth mortar was weighted and placed in an oven to dry. The water content was determined by the difference in weight of fresh mortars samples and the same samples after oven dried.

The top and bottom surfaces of some of the simple compression adobe specimens, as well as the ones with the overlapped adobe with bedding mortar were not perfectly regular. Therefore a capping performed by a thin layer of 1:3 volumetric proportion of cement:sand mortar was applied in all the top and bottom compression specimens (surfaces of simple prisms - Figure 7a - and overlapped specimens that would be in contact with the compression equipment plates - Figure 7b) to assure complete contact of the area that would be in contact with the press plates.

All the masonry samples were left in a controlled T and RH environment for a period of 8 days, to make sure that the mortar was tough enough to proceed with the tests.

The capillarity test was performed based on the EN 15801 (2009) but caution was taken to avoid the loss of mass during the test. Based on Lima et al. (2019) and to reduce particle loss, the base

and lateral surfaces of specimens were enveloped in a water vapor permeable synthetic fabric, with small openings, invisible to the open eye , and with low water absorption. To avoid direct handling of the specimens and prevent the degradation during the weighing, the specimens were placed inside metallic net baskets. With the objective of maintaining constant contact with water during the test, sponge cloths with 2 mm of thickness drenched in water were used. Due to the variation in the specimen dimensions in contact with water, AutoCAD software was used to measure the face exposed to water. The weighing's were performed with a precision scale of 0.01 g, for the first 40 min with time intervals of 5 min. The subsequent measurements were at 60 min, 90 min, 180 min, 300 min, 1440 min and ended at the 2880 min mark. Through the capillarity curves it was possible to compare the behavior of the specimens and calculate the coefficient of capillary absorption (Cc), in kg/(m². min½). After the specimens had achieved the saturation through the capillarity test, the drying test started. It was performed at the same conditions of T and RH and weightings were taken, until the difference between the initial and final dry masses was stabilized. The drying occurred by the superior and lateral faces, which were measured with the help of AutoCAD. The weighing was made with time intervals of 10 min in the first hour, than1 hour and finally 24 hours. The same scale was used. The results are presented by two types of drying curves, with ordinates representing the loss of water mass, in kg/m², and abscissae with the time in hours or the square root of hour. The drying rates are calculated by the slope of linear parts of the drying curves. The drying rate, DR1 kg/m².h, represents the drying in an initial phase, which occurs mainly through the transportation of liquid water to the surface of the material. The drying rate TS2, in kg/m².h, represents a diminishing phase of the transportation of liquid water with a rise in the diffusion of the water vapor (Gonçalves et al., 2015).

3. Results and discussion

3.1 Dry particle size distribution, quick sedimentation and XRD of adobe material

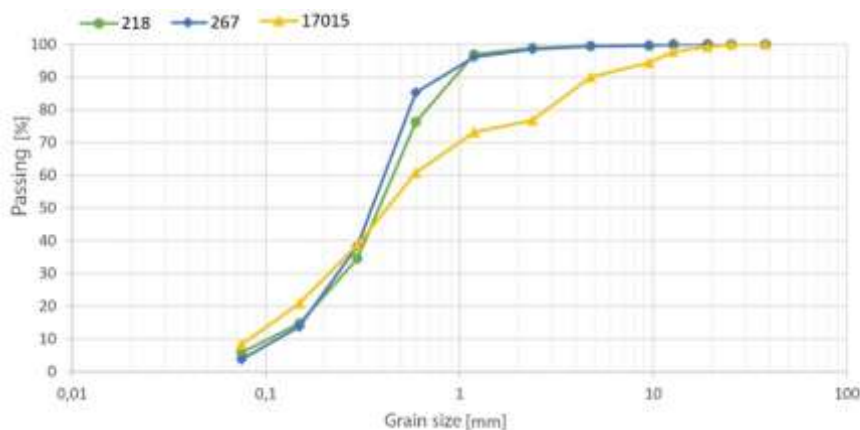Dry particle size distribution curves of the adobe material are presented in Figure 8.

Figure 8. Dry particle size distribution curves.

Case studies 218 and 267 percentage of coarse material is lower than 1% but 15% is obtained for dwelling 17015. In all samples, sand is predominant, in a similar way to the vernacular adobe of Nisa Partica, in Turkmenistan, studied by Adorni, Coisson and Ferretti (2013) and the percentages of scrap were significative, showing the presence of a fine material.

According to Costa et al. (2019) and concerning the particle size distribution, adobe can be divided into three groups: fine adobes, that show very low to no presence of sand; medium adobes, characterized by sand varying from 0.063-2 mm; coarse adobes, with aggregates that include pebbles. Case studies 218 and 267 present a very high content of sand and may be classified as medium adobes while case study 17015 revealed a large percentage of coarse aggregates and as such it is possible to include it in the third group (coarse adobe).

Regarding the expedited sedimentation in jar test (Figure 9), case study 17015 is the one that shows the largest percentage of sand, with a value of 63 %.
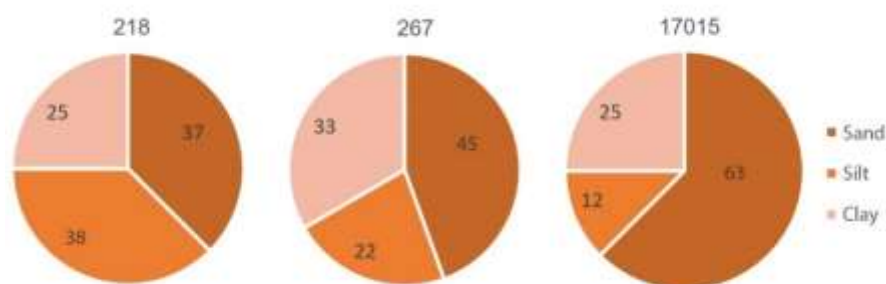

Figure 9. Distribution of sand, silt and clay on adobe case studies by the quick jar sedimentation test.

As was the case with the dry particle size distribution, this test confirms that the predominant material in the adobe of the Caramel dwellings, from Pinhal Novo and Moita, is sand, followed by clay, except for adobe from case study 218 where the silt is preponderant to clay.

Castrillo, Philokyprou and Ioannou (2017) showed larger percentages of fine particles (70% of fine particles) for pre-historic adobes produced in Cyprus, far superior to the values obtained in the present study. Cyprus adobe had coarse aggregates with an average of 24%, inferior to the ones obtained in the present study.

The results of particle size distribution curves obtained by the dry sieving of the adobes' disaggregated materials (Figure 8) indicate that the percentage content in silt and clay (particles < 0.075 mm) is in all cases less than 10%. However, results obtained from jar sedimentation tests (Figure 9) indicate contents in silt and clay higher than 35%. This is an evidence that the dry particle size distribution alone is not representative of the adobe material particle size because fine particles can be agglomerated and considered as coarser particles. Therefore, when the wet particle size distribution is not possible to be performed and the dry test is the possible solution, there is a need to complement it with other tests for fine particles. In the present case the dry particle size

distribution should only be considered for the coarser particles. For finer particles, such as silt and clay, the qualitative proportion of the jar test should be considered.

Results of XRD of adobe samples can be consulted in Table 4.

Table 4. Results of adobe material characterization by XRD.

Specimen	Quartz [%]	Kaolinite [%]	Microcline [%]	Albite [%]	Muscovite [%]
218	84.9	0.4	5.5	8.0	1.5
267	76.0	1.6	15.7	3.4	3.4
17015	86.6	0.5	9.3	-	3.6

The diffractograms resulting from the tests on the different adobes showed that the predominant material is quartz, accompanied by feldspars (i.e. albite and microcline) as it was expected in a sandy material. The presence of kaolinite and muscovite was noticed. Based on Costa et al. (2019), kaolinitic clay is associated with higher mechanical strength and water absorption by earthen materials. This might justify the fact that Parracha et al. (2019) found lower mechanical strength for a vernacular unstabilized rammed earth sample (T3) that did not have kaolin, in comparison to other unstabilized samples. Adobe samples in the study of Leiria (Parracha et al., 2019) further confirm this theory, with sample A1, that showed traces of kaolinite in the XRD, against no presence in samples A2 and A3, showing much better values of compressive and tensile strength, as well as much higher values of thermal conductivity (0.69 ± 0.13 W/(m.K) from sample A1 against 0.41 ± 0.04 W/(m.K)).

Miccoli et al. (2014) and Fratini et al. (2011) also analyzed the mineralogic composition of adobes by XRD and concluded that the presence of kaolinite is recurring, while Abanto et al. (2017) identified the presence of montmorillonite, apart from quartz and feldspar.

3.2 Color

From the evaluation through the colorimeter (Table 5) the adobes from case studies 218 and 267 are the most similar. Case study 17015 showed significantly different values, which was already confirmed through visual observation (Table 2).

Table 5. Evaluation of color by colorimeter.

Adobe	218	267	17015
CIELAB coordinates	L*- 51.89 a*- 5.14 b*- 15.95	L*- 53.55 a*- 3.43 b*- 13.70	L*- 47.99 a*- 8.59 b*- 16.81

3.3 Bulk density and ultrasonic pulse velocity

The adobes of the three case studies show very similar values for bulk density, as can be seen on Table 6. However, 267 and 17015 adobes present higher bulk densities in comparison to specimens that belong to case study 218. The higher bulk density of 17015 adobe may be justified by the

coarser aggregates in its composition. Samples from case study 267 show a standard deviation far superior to the other samples which confirms the higher heterogeneity of the material that was previously visualized.

Table 6. Adobe characterization - average values and standard deviation.

Test	218	267	17015	Global
Bulk density, ρ [kg/m³]	1792 ±156	1784±423	1792±176	1764±268
Ultrasonic Pulse Velocity, Vus [m/s]	808±235	720±181	647±275	725±66
Superficial hardness [Shore A]	70±11	64±12	66±12	67±0.44
Mass loss by dry abrasion [g]	3.7±1.4	5.8±1.5	3.3±0.8	4.3±1.7
Thermal conductivity, λ [W/(m.K)]	0.68±0.15	0.56+0.19	0.67±0.22	0.63±0.03
Flexural strength [N/mm²]	0.65±0.32	0.31±0.10	0.31±0.08	0.44±0.27
Compressive strength - simple test, CStr [N/mm²]	1.12±0.40	0.58±0.07	0.78±0.15	0.85±0.34
Compressive strength - adobe with mortar masonry, CStr_m [N/mm²]	0.52±0.17	0.31±0.05	0.52±0.11	0.45±0.16
Capillarity absorption, Cc [kg/(m².min½)]	0.39	0.56	0.12	0.36±0.18
Drying rate phase 1, DR1 [kg/(m².h)]	0.07±0.01	0.18±0.8	0.06±0.04	0.15±0.03
Drying rate phase 2, DR2[kg/(m².h$^{1/2}$)]	0.41±0.07	0.58±0.2	0.29±0.06	0.43±0.04

Parracha et al. (2019), for vernacular unstabilized adobe of Leiria region, obtained average values of 1730 ± 60 kg/m³ and 1400 ± 50 kg/m³, similar to values obtained by Silveira et al. (2016) for stabilized adobe in the Aveiro region (Table 1). These values are both lower and higher than the ones obtained for Caramel´s adobe, being generally higher, with a global value of 1764 ± 268 kg/m³ for the three case studies. Nevertheless, Abanto et al. (2017), when characterizing adobe from rural regions of Peru, achieved an average of 1716 kg/m³ with the same method used in the present study, being these values very close to the ones found in the testing of Caramel adobe samples.

It can be observed that the ultrasonic pulse velocity of adobe is inversely proportional to their bulk density. One of the possible explanations for this might be that case study 17015 adobe, by having a higher percentage of large dimension aggregates, may present more discontinuities between the matrix and the coarse aggregates. The unstabilized adobe of Leiria region tested by Parracha et al. (2019) presented much lower ultrasonic pulse velocity and much higher dispersion, with 921.1 ± 262.7 m/s for adobe sample 1, 339.4 ± 46.8 m/s for adobe sample 2 and 272.5 ± 36.5 m/s for adobe sample 3, in comparison to the present study (global value of 725 ± 66 m/s - Table 6).

3.4 Thermal conductivity

Results for thermal conductivity are presented in Table 6 and the adobes from case study 218 and 17015 present the highest values. Case study 17015 is the one that has the largest percentage of sand (Figure 9), as well as the one that shows the highest bulk density, being this characteristic usually associated with higher thermal conductivity. Parracha et al. (2019) obtained values for unstabilized adobe between 0.69 ± 0.13 W/(m.K) and 0.41 ± 0.04 W/(m.K), which is even lower in comparison to the global value of 0.63 ± 0.03 W/(m.K) registered in the present study. For adobe

in a the region of Peru characterized by Abanto et al. (2017) there is an average value of 0.30 W/(m.K).

A document accepted by the Portuguese thermal legislation (Pina dos Santos and Matias, 2006) defines that for earthen construction, like adobe, the value of thermal conductibility, λ, of 1.10 W/(m.K) should be considered, which is much higher than the global value of 0.63 W/(m.K) obtained for the Caramel´s adobe (Table 6). These lower values of λ can therefore be used to support thermal calculation and achieve more efficient thermal transmittance values (U-value) when retrofitting this type of vernacular dwellings.

Pinhal Novo and Moita are located in the Portuguese thermal climatic zone I1, the most favorable (Portuguese Republic, 2013) and the maximum U-value corresponding to that zone is 0.50 W/(m^2.K) (Portuguese Republic, 2015). For case study 218, with an adobe wall of 0.33 m thickness and thermal conductivity of 0.68 W/(m.K), with an air lime or lime-earth outdoor render and indoor plaster with 0.015 m thickness each, considered with a thermal conductivity of 0.58 W/(m.K) (Faria et al., 2014), the U-value is 1.41 W/(m^2.K) which is much higher than the maximum U-value. Nevertheless, the solid adobe masonry walls provide a much higher thermal inertia in comparison to common hollow brick masonry walls, and that aspect is not taken into consideration by the thermal legislation that classifies both masonries as "high thermal inertia".

3.5 Mass loss by dry abrasion

Results of weight loss by dry abrasion are presented in Table 6. The specimens that suffered the highest mass loss were the ones that belong to case study 267, which means that they have a lower resistance to abrasion and are prone to suffering more damage when they are not protected by a render on the exterior envelope, or a plaster when indoors. The samples that had the lowest mass loss are the samples from dwelling 17015, which may be justified by the higher content of coarser aggregates in comparison to the other adobes.

The global weight loss of the three adobe case studies is 4.3 g (Table 6), much lower than the average of 14.0 g registered by Parracha et al. (2019), also for unstabilised adobe but from the Leiria region.

3.6 Flexural and compressive strength

Results of flexural and compressive strength are presented in Table 6. The type of failure resulting from the simple compression test can be seen in Figure 10.

Figure 10. Failure obtained in simple compressed specimens, similar to concrete explosive failure (EN 12390-3, 2019)

The result obtained for flexural strength for 218 adobe is compatible with results from previous testing (ultrasonic pulse velocity and bulk density), showing the best cohesion and homogeneity, which in turn translates into higher flexural strength. For flexural strength, adobe specimens in the present study showed average values of 0.44 N/mm^2, although with a high standard deviation (Table 6).

Comparing to Table 1, it seems that the unstabilized adobe from Moita and Pinhal Novo have similar flexural strength to stabilized adobe of Aveiro (Figueiredo et al., 2013) and significantly higher values in comparison to unstabilized adobe from Leiria (Parracha et al., 2019). Therefore, it seems that the type of earth and the moulding procedures may have more influence on the values obtained for flexural strength, rather than the stabilization itself.

Observing the fracture sections of samples after simple compressive tests, case study 267 seems to present lower cohesion, with large dimension voids, which also translates into lower values of compressive resistance (Table 6).

For the simple compressive strength, CStr (Table 6), all adobe samples have a global value and standard deviation of 0.85±0.34 N/mm^2 , and values between 1.12±0.40 N/mm^2 and 0.58±0.07 N/mm^2 , very close to the values between 1.06 ± 0.22 N/mm^2 and 0.69 ± 0.35 N/mm^2 obtained by Parracha et al. (2019) (Table 1). The coefficient of variation in the present study is of 40%, lower than the coefficient of variation obtained, for example, by Coroado et al. (2010).

In comparison, Costa et al. (2013) obtained higher values than the present study, with average values of 2.52 N/mm^2 in the region of Anadia and 1.76 N/mm^2 in Murtosa (Silveira, Varum and Costa, 2013) showing average values for cubic specimens of air lime stabilized adobe of 0.28 N/mm² and a value for coefficient of variation of 0.47%. Other studies from Aveiro (Coroado et al., 2010) showed compressive strengths between 0.41 N/mm^2 and 1.44 N/mm^2, with an average low value of 0.50 N/mm^2 (Table 1).

The compressive strength for both the previous studies is lower than the values obtained in the present study, which means the earth of the region of Pinhal Novo and Moita might have properties

that confer it higher compressive strength than unstabilized and stabilized adobe from other Portuguese regions.

For Cyprus adobe Illamas, Ioannou and Charmpis (2014) obtained average values of 1.15 N/mm^2 with a value for coefficient of variation of 0.36% for cubic specimens, which are closer to the ones obtained in the present study, with adobe that has the presence of fibers. Illampas, Ioannou and Charmpis (2014) also showed average values of 1.53 N/mm^2 for prisms and 1 N/mm^2 for cylindric specimens, showing that the type of sample may have an important influence on compressive strength results.

The water content of the earth mortars used as bedding mortar, for the compressive strength specimens composed by two overlapped adobe samples, is presented in Table 7. Bedding mortars should be weaker than adobe to allow deformation of the structure without damaging the adobe, as well as having a water vapour permeability similar to the one obtained by adobe, contributing towards their durability. As mentioned before, these mortars were produced with the same earth as the adobes that composed the walls, even though they had a more careful selection of grain size, with removal of the larger particles in the gravel range, due to the low thickness of the bedding mortar (less than 2 cm). Although the earthen materials are different, is possible to observe that their water content is quite similar and, therefore, that may not influence results.

Table 7. Water content for earth bedding mortars for producing the adobe masonry test specimens.

Mortar	218	267	17015
Water content (%)	16	18	17

This proximity of water content to achieve adequate workability for the mortars to be applied as bedding mortars can be justified by the similar mineralogic composition of the different earths, all mainly kaolinitic.

It can be observed that the adobe masonry specimen from case study 267 presents the lowest compressive strength, on the same tendency shown by the simple compression test. Similar results were obtained for adobe specimens belonging to case studies 218 and 17015.

Comparing the results of the adobes tested simulating the masonry and the simple adobe, it stands out that the latter test conducts to incremented values of compressive strength: 115% for 218 adobe, 87% for 267 adobe and 152% for 17015 adobe, which was expected. It can also be observed that the average compressive strength of adobe masonry (0.38 N/mm^2) is higher in comparison with the simple adobe compressive strength.

3.7 Capillarity and drying

Figure 11 presents the capillarity curves for all case studies, resulting from the average of each test specimens. It presents an initial phase of absorption, in which it is possible to calculate the coefficient, Cc, in kg/(m².min½), in the time frame corresponding to the first minutes of test.
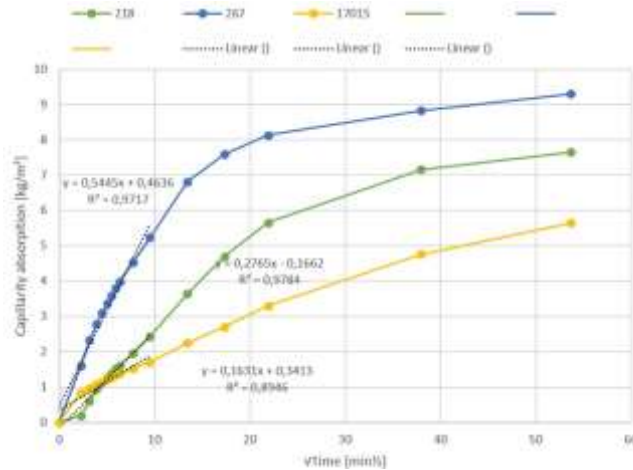

Figure 11. Average capillarity curves of adobe samples with the slope of the most representative absorption segments.

The Cc for each case study is registered in Table 6, resulting from the respective slope. Adobes from case study 17015 (Figure 11, Table 6) are the ones with the lowest Cc, while case study 267 presents the highest Cc. As an example representative to all case studies, Figure 12 presents the capillary curves of the four specimens from case study 218 that were tested for capillarity water absorption.
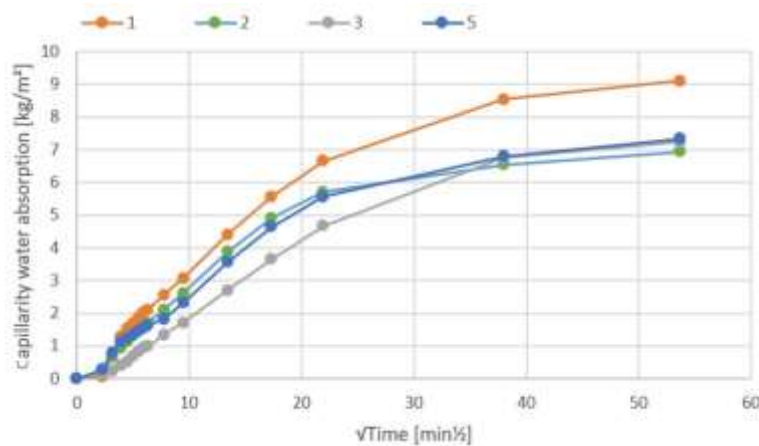
Figure 12. Initial part of capillarity curves of all the samples of adobes from case study 218.

It can be observed that the capillary absorption is not uniform during the first minutes: there is an initial low slope and only after this does the slope increases for all the samples. The same initial behavior was registered for unstabilized kaolinitic earth mortars by Gomes, Gonçalves and Faria (2016) which depicted nonlinear (exponential) dependence on the square root of time during the first minutes, rather than the expected linear dependence. This may be justified by a reduction of

pore size right after the contact of the clayish earth with water, raising the quantity of active capillary pores and promoting a faster capillary absorption. The low clayish content of the earth of case study 17015 might justify the low Cc obtained for case study 17015.

Parracha et al. (2019), for unstabilized adobes from Leiria region, presented a much higher capillary absorption coefficient (average of 0.71 kg/(m^2.min$^{1/2}$)) in comparison to rammed earth samples from the same region (average of 1.30 kg/(m^2.min$^{1/2}$)), and also in comparison to Caramel´s adobe (average of 0.36 kg/(m^2.min$^{1/2}$) - Table 6). This behavior of Caramel´s adobe is very positive and might be related to characteristics of unstabilized earth that affects the absorption, such as the type and content of clay.

Figures 13 and 14 show the drying curves resulting from the drying test of the adobe samples of each case study. As an example, Figures 15 and 16 presents the drying curves of all the specimens from case study 218 that were tested for drying.
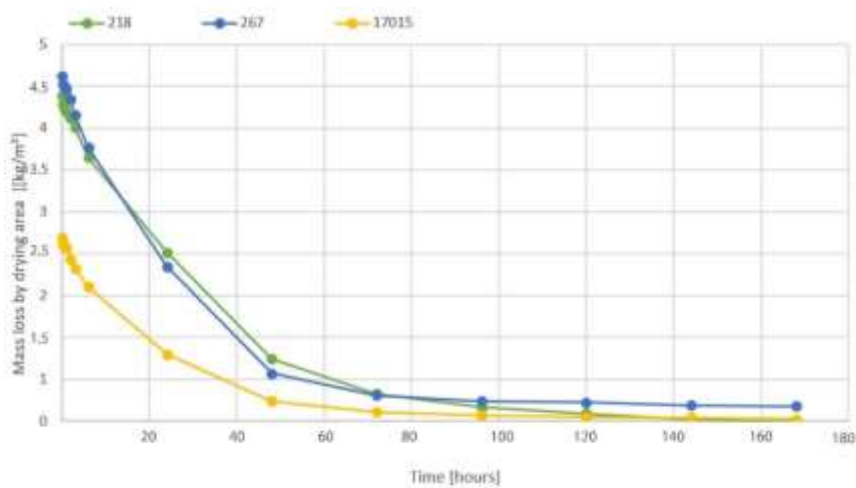

Figure 13. Drying curves of averaged experimental results of adobe samples with the X axis in time, with the slope of the initial drying segments.
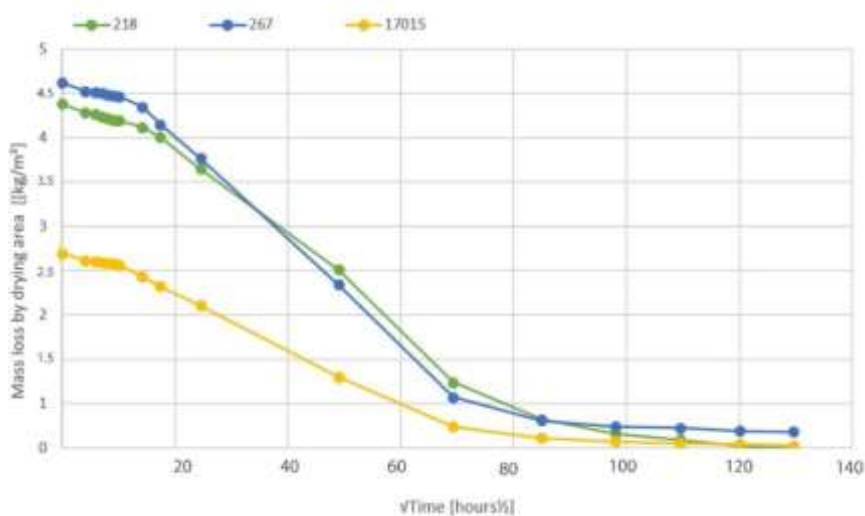

Figure 14. Drying curves of averaged experimental results of adobe samples with the X axis in square root of time, with the slope of intermediate drying segments.
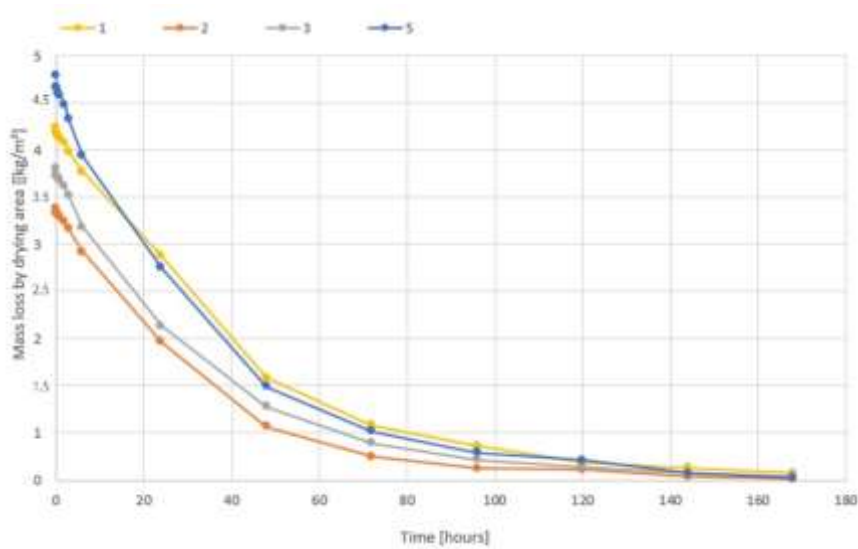
Figure 15. Drying curves of all the adobe samples from case study 218 by time.
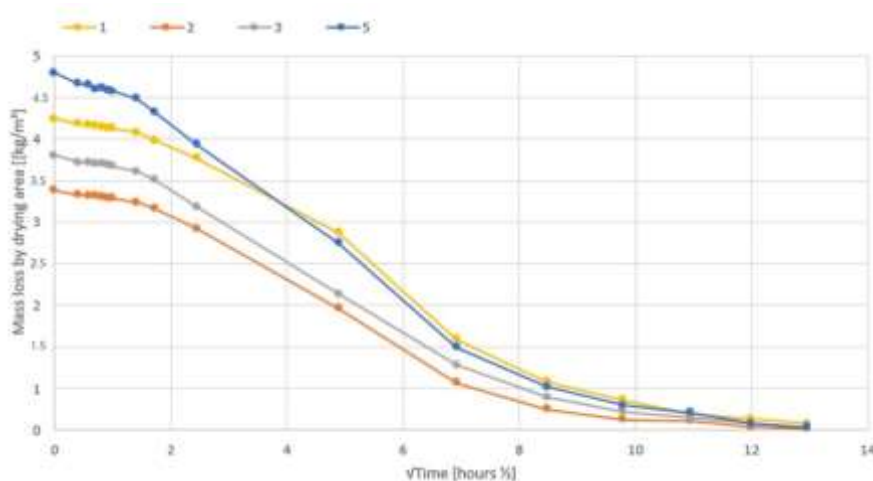

Figure 16. Drying curves of all the adobe samples from case study 218 by square root of time.

The segments that allow the assessment of the drying rates on the first and second drying phases of all case studies are represented in the same figures (Figures 13 and 14, respectively), and calculated drying rates are registered in Table 6. Adobes that belong to case study 267 have the highest drying capacity in both phases, which is important since they also had the highest Cc. In the opposite spectrum 17015 adobe, that presented the lower Cc, presents now the lowest drying capacity in both drying phases. The results of case study 17015 might be justified by the higher bulk density, which also affects the ultrasonic pulse velocity, and might decrease the potential of water absorption and drying.

Unstabilized adobes from Leiria tested by Parracha et al. (2019) show similar to lower drying rates in comparison to rammed earth samples in the same region, both with 0.12 kg/(m².h) for phase 1and 0.47 kg/(m².h½) and 0.54 kg/(m².h½) for phase 2, respectively. The drying rates for adobe from Leiria are once again similar to the ones obtained of Caramel´s adobe (Table 6). As the

Caramel´s capillarity coefficient is lower, that similar drying capacity is very positive, indicating that moisture that accesses that wall by capillary rise, indoor activities or rain may be dried faster, having in account that it is not blocked by a water vapor barrier, such as an incompatible render, as is the case of cement based renders that are wrongly applied in the rehabilitation of many of these buildings.

Case study 17015 shows the lowest drying rate, ultrasonic pulse velocity and capillary absorption, as well as the highest bulk density, thermal conductivity, flexural and compressive strength. Case study 17015 also shows the highest percentage of sand and lowest percentage of clay. It is easily understood why a higher density can lead to higher thermal conductivity, UPV and compressive strength. As mentioned previously, the lower capillary coefficient and drying rate, particularly in the second phase when drying is mainly by vapor transport (Brito, Gonçalves and Faria, 2011) and might be connected to the lower content of clay. Therefore, a higher clay content may be related to a faster capillary absorption but also drying (particularly in the second phase of drying) on unstabilized earth construction. In any case, it seems important that plasters, renders and paint systems do not eliminate this drying capability (Brito, Gonçalves and Faria, 2011). Again, clay and air lime-based mortars and paints should be used in the rehabilitation to protect the Caramel dwellings.

4 Conclusions

Although there are a large number of vernacular adobe buildings in Portugal, and in many other regions of the world, very few material characterization is available to support the interventions. There is a strong need for the characterization of adobe materials from existing constructions by experimental methods because the properties associated with the adobe performance can support decisions on the conservation and rehabilitation of these structures.

Any data could be found on Caramela dwellings adobe characteristics. This fact justifies the need of material characterization for the Caramel's dwellings, having in mind their possible rehabilitation.

The present study also shows there is a lack of standards that can be applied to characterize historic adobe masonry constructions. Test standards could contribute to homogenize procedures, facilitate comparison and increase knowledge on this method of earth construction.

Laboratory testing was performed on adobe samples picked from three case studies. The original adobes were tested for bulk density, ultrasonic pulse velocity, thermal conductivity and, after being cut, specimens were tested for dry abrasion, flexural and compressive strength, capillary absorption and drying.

The laboratory tests revealed that the clayish earth used to produce adobes in Pinhal Novo and

Moita is mainly kaolinitic. The Caramel´s adobes are not air lime stabilized (which means they are not lime adobe as can be found in the Aveiro region, Portugal). Nevertheless, they have comparable or even higher strength than vernacular lime adobes characterized by other researchers.

Although limited to samples of only three case studies, higher values of bulk density, thermal conductivity, ultrasonic pulse velocity and compressive and flexural strength might be justified by higher sand content, while higher capillary water absorption coefficient and drying rates might be justified by a higher clay content in the adobes.

The thermal conductivity of these vernacular adobes is lower and more favorable than the values stipulated by a supporting document to the Portuguese thermal regulation. The thermal design and energy certification should not only consider the thermal conductivity and adobe masonry U-value but also the high thermal inertia and high hygroscopic properties of these masonries.

A wider study should be done in the near future to extend the characterization to more dwelling case studies, with the objective of achieving a more accurate characterization.

At the end of their life cycle, unstabilized adobes masonries are easily reintegrated in the environment, reducing to zero the debris, which is a very positive characteristic of this type of construction. All these facts highlight the potential in proceeding with the conservation and rehabilitation of some of these dwellings to preserve this cultural vernacular heritage and the data obtained can contribute to support the design of repair interventions.

Disclosure

No potential conflict of interest was reported by the authors.

Funding/Acknowledgements

ORCID

José Mirão - https://orcid.org/0000-0003-0103-3448

Paulina Faria - https://orcid.org/0000-0003-0372-949X

References

Abanto, G.A., M. Karkri, G. Lefebvre, M. Horn, J. Solis, M.M. Gómez, 2017. Thermal properties of adobe employed in Peruvian rural areas: Experimental results and numerical simulation of a traditional bio-composite material. Case Studies in Construction Materials 6:177–91, doi: 10.1016/j.cscm.2017.02.001.

Adorni, E., E. Coisson, D. Ferretti, 2013. In situ characterization of archaeological adobe bricks. Construction Materials 6 :16-28, doi: 10.1016/j.Cscm.2016.11.003.

ASTM D2240-15e1, 2015. Standard test method for rubber property - Durometer hardness. ASTM International, West Conshohocken, PA.

ASTM D5930-17, 2017. Standard test method for thermal conductivity of plastics by means of a transient line-source technique. ASTM International, West Conshohocken, PA.

Beckett, C.T., Jaquin, P.A., Morel, J.-C. (2020), Weathering the storm: A framework to assess the resistance of earthen structures to water damage. Construction and Building Materials 242: 118098, doi: 10.1016/j.conbuildmat.2020.118098.

Brito, V., T.D. Gonçalves, P. Faria, 2011. Coatings applied on damp substrates: performance and influence on moisture transport. Journal of Coating Technology and Research 8 (4):513-525, doi:10.1007/s11998-010-9319-5.

Bruno, P., 2007. Earth architecture in pre-history – Remains of domestic structures, from the 6th to the 2nd millenia B.C., in south Portugal. Terra em Seminário 2007. Lisbon: Argumentum, 149-152 (in Portuguese).

Bui, Q.-B., Morel, J.-C. (2015), First exploratory study on the ageing of rammed earth material. Materials 8:1-15, doi:10.3390/ma8010001.

Caporale, A., F. Parisi, D. Asprone, R. Luciano, A. Prota, 2015. Comparative micromechanical assessment of adobe and clay brick masonry assemblages based on experimental data sets. Composite Structures 120:208-220, doi: 10.1016/j.compstruct.2014.09.046.

Coroado, J., H. Paiva, A. Velosa, V. M. Ferreira, 2010. Characterization of renders, joint mortars, and adobes from traditional constructions in Aveiro (Portugal). International Journal of Architectural Heritage 4 (2):102–14, doi:10.1080/15583050903121877.

Costa, C., F. Rocha, H.Varum, A.Velosa, 2013. Influence of the mineralogical composition on the properties of adobe blocks from Aveiro. Portugal. Journal of Clay Minerals 48 (5):749–58, doi: 10.1180/claymin.2013.048.5.07.

Costa, C., Â. Cerqueira, F. Rocha, A. Velosa, 2018. The sustainability of adobe construction: Past to future. International Journal of Architectural Heritage, doi:10.1080/15583058.2018.1459954.

Costa, C., D. Arduin, F. Rocha, A. Velosa, 2019. Adobe blocks in the center of Portugal: Main characteristics, International Journal of Architectural Heritage, doi: 10.1080/15583058.2019.1627442

Castrillo, M., M. Philokyprou, I. Ioannou, 2017. Comparison of adobes from pre-history to date. Journal of Archaeological Science 12:437–48, doi: 10.1016/j.jasrep.2017.02.009.

DIN 18947, 2013. Earth plasters - Terms and definitions, requirements, test methods. Berlin, NABau (in German).

EN 1015-1, 1999. Methods of test for mortar for masonry. Determination of particle size distribution (by sieve analysis), Brussels, CEN.

EN 1996-1-1, 2005. Eurocode 6 - Design of masonry structures - Part 1-1: General rules for reinforced and unreinforced masonry structures. Brussels, CEN.

EN 12390-3. 2019. Testing hardened concrete. Part 3: Compressive strength of test specimens. Brussels, CEN.

EN 12504-4. 2004.Testing concrete. Determination of ultrasonic pulse velocity. Brussels, CEN.

EN 15801, 2009. Conservation of cultural property. Test methods – Determination of water absorption by capillarity. Brussels, CEN.

EN 16322, 2013. Conservation of cultural property. Test methods – Determination of drying properties. Brussels, CEN.EN 12390-3, 2019. Testing hardened concrete. Part 3: Compressive strength of test specimens. Brussels, CEN.

Fabbri, A., McGregor, F., Costa, I., Faria, P. (2017), Effect of temperature on the sorption curves of earthen materials. Materials and Structures 50, 253, doi: 10.1617/s11527-019-1316-2.

Faria, P., V. Silva, N. Jamú, I. Dias, M.I. Gomes, 2014. Evaluation of air lime and clayish earth mortars for earthen wall renders. Vernacular Heritage and Earthen Architecture: Contributions for Sustainable Development, Correia, Carlos & Rocha (Eds). Taylor & Francis Group, 407-413.

Fernandes, M., 2008. The settlers and adobe architecture in Portugal. TerraBrasil 2008, VII SIACOT, UEMA PROTERRA, 272-280 (in Portuguese).

Figueiredo, A., H. Varum, A.Costa, D. Silveira, C. Oliveira, 2013. Seismic retrofitting solution of an adobe masonry wall. Materials and Structures 46:203-219, doi:10.1617/s11527-012-9895-1.

Fratini, F., E. Pecchioni, L. Rovero, U. Tonietti, 2011. The earth in the architecture of the historical centre of Lamezia Terme (Italy): Characterization for restoration. Applied Clay Science 53:509–16, doi:10.1016/j.clay.2010.11.007.

Gomes, M., T. Gonçalves, P. Faria, 2016. Hydric behavior of earth materials and the effects of their stabilization with cement or lime: Study on repair mortars for historical rammed earth structures. Journal of Materials in Civil Engineering 28: 04016041, doi:10.1061/(ASCE)MT.1943-5533.0001536.

Gonçalves, T., V. Brito, F. Vidigal, L. Matias, P. Faria, 2015. Evaporation from porous building materials and Its Cooling Potential. Journal of Materials in Civil Engineering 27 (8):04014222, doi:10.1061/(ASCE)MT.1943-5533.0001174.

Hubbard, C. R., E. H. Evans, D. K. Smith, 1976. The reference intensity ratio, I/Ic, for computer simulated powder patterns. Journal of Applied Crystallography 9(2):169-174, doi: 10.1107/S0021889876010807.

Illampas, R., I. Ioannou, D.C. Charmpis. 2014. Adobe bricks under compression: Experimental investigation and derivation of stress–strain equation. Construction and Building Materials 53:83–90, doi: 10.1016/j.conbuildmat.2013.11.103.

Lima, J., Faria, P., Santos Silva, A. (2019), Earth plasters: the influence of clay mineralogy in the plasters' properties. International Journal of Architectural Heritage, doi: 10.1080/15583058.2020.1727064.

Miccoli, L., U. Müller, P. Fontana, 2014. Mechanical behaviour of earthen materials: A comparison between earth block masonry, rammed earth and cob. Construction and Building Materials 61:327–39, doi:10.1016/j.conbuildmat.2014.03.009.

NTC 5324, 2004. Bloques de suelo cemento para muros y divisiones. definiciones. especificaciones. metodos de ensayo. condiciones de entrega. ICONTEC, Colombia.

NTE.E.080, 2017. Diseño y construcción con tierra reforzada. Ministerio de Vivienda, Construcción y Saneamiento, Peru.

Parracha, J., J. Lima, M. Freire, M. Ferreira, P. Faria, 2019. Vernacular earthen buildings from Leiria, Portugal – material characterization. International Journal of Architectural Heritage, doi: 10.1080/15583058.2019.1668986.

Pina dos Santos, C., L. Matias, 2006. U-values of building envelope elements. ITE 50, Lisbon, LNEC (in Portuguese).

Portuguese Republic, 2013. Despacho 15793-F, DR, 2ª serie, nº 234 (in Portuguese).

Portuguese Republic, 2015. Portaria 379-A, DR, 1ª serie, nº 207 (in Portuguese).

Sampaio, T., I. Oliveira, P. Faria, 2017. The Caramela dwelling – the immateriality of the matter. M. Menezes, D. Costa, J. Delgado Rodrigues (Eds.), IMaTTe 2017 - International Conference on the Values of Tangible Heritage. Lisbon: LNEC, 345-354.

Silveira, D., H. Varum, A. Costa, T. Martins, H. Pereira, J. Almeida, 2012. Mechanical properties of adobe bricks in ancient constructions. Construction and Building Materials 28:36-44, doi: 10.1016/j.conbuildmat.2011.08.046.

Silveira, D., H. Varum, A. Costa, 2013. Influence of the testing procedures in the mechanical characterization of adobe bricks. Construction and Buildings Materials 40:719-728, doi:10.1016/j.conbuildmat.2012.11.058.

Silveira, D., H. Varum, A. Costa, C. Neto, 2016. Survey of the facade walls of existing adobe buildings. International Journal of Architectural Heritage 10(7):867–86, doi: 10.1080/15583058.2016.1154114.

Walker, P., 2002. The Australian earth building handbook, HB195–2002. Sydney: Standards Australia.

W1 - http://dbheritage.lnec.pt/ (accessed 13/12/2019)